

## Long-term memory at the onset of noise-induced chaos synchronization

Kazuyuki Yoshimura, Peter Davis, and Jun Muramatsu

NTT Communication Science Laboratories, NTT Corporation  
2-4, Hikaridai, Seika-cho, Soraku-gun, Kyoto 619-0237, Japan  
Email: { kazuyuki, davis, pure }@cslab.kecl.ntt.co.jp

**Abstract**—We study the time for decay of information about initial conditions in one-dimensional chaotic maps that exhibit noise-induced chaos synchronization. We found that the decay time becomes maximum at the onset of noise-induced chaos synchronization.

### 1. Introduction

In a chaotic dynamical system, information about the initial conditions is gradually lost during its time evolution: any localized initial probability distribution converges to the invariant probability distribution, which is independent of the initial distribution. The decay of information about the initial conditions and, in particular, the time needed for the decay, which we call the *memory decay time*, depends on the system. For example, two very different types of the decay processes were observed for the logistic map and the Belousov-Zhabotinsky map in Refs. [1, 2].

In the present paper, we consider one-dimensional chaotic maps with external noise inputs. It is known that for some chaotic systems a common noise input to two independent and identical systems could give rise to the synchronized motion of the two systems [3, 4]. We call this phenomenon *noise-induced chaos synchronization* (NICS). Toral *et al.* constructed some one-dimensional chaotic maps and demonstrated that for those maps the NICS occurs when a bifurcation parameter exceeds a threshold value [3]. The NICS in coupled chaotic maps was shown to occur in Ref. [4]. In this study, we focus on noise-synchronizable chaotic maps and investigate how the memory decay time depends on the bifurcation parameter that controls the transition to the NICS. We show that the memory decay time is maximized at the transition point. This is an example of an anomalous behavior which can occur at a transition point to the NICS.

The present paper is organized as follows. In Sec. 2, we introduce two chaotic map models and show that these maps exhibit NICS. In Sec. 3, we show that for a noise-driven chaotic map any two different initial probability distribution converge to the same time-dependent probability distribution as the map is iterated. To characterize the decay of information about the initial conditions, we introduce the mutual information and define the memory decay time. In Sec. 4, numerical results on the memory decay time are shown. In addition, we discuss the reason why the memory decay time is maximized at the transition point to

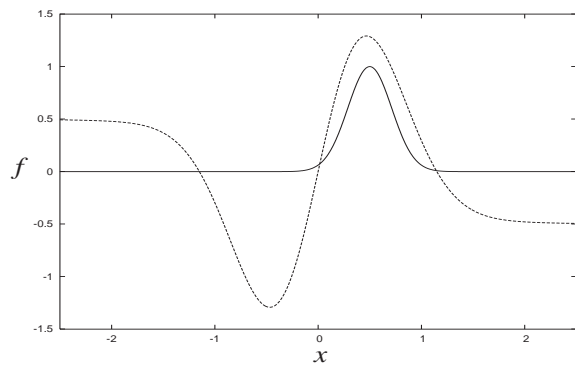


Figure 1: Shapes of map functions (2) (solid line) and (3) (dashed line).

the NICS. Conclusions are drawn in Sec. 5,

### 2. Chaotic maps and noise-induced chaos synchronization

Our investigation is of one-dimensional chaotic maps of the form

$$x_{n+1} = f(x_n) + \sigma \xi_n, \quad (1)$$

where  $x_n \in \mathbf{R}$  is the state variable depending on the time index  $n$ ,  $\xi_n$  represents the time-dependent noise uniformly distributed in the interval  $[-1/2, 1/2]$  and uncorrelated in time, and  $\sigma$  is the noise amplitude. As for the map function  $f$ , we consider two examples. The first one is

$$f(x) = \exp \left[ - \left( \frac{x - 1/2}{\omega} \right)^2 \right], \quad (2)$$

where  $\omega$  is a constant and we set  $\omega = 0.3$ . This map was proposed in Ref. [3] for demonstrating the NICS. The other one is

$$f(x) = ax \exp(-bx^2) - c \tanh(x), \quad (3)$$

where  $a$ ,  $b$ , and  $c$  are constants. We assume  $a = 5$ ,  $b = 2$ , and  $c = 1/2$ . The shapes of these maps are shown in Fig. 1.

Consider two trajectories  $x_n$  and  $y_n$  of map (1) with the initial conditions  $x_0$  and  $y_0$  for the same realization of the noise sequence  $\xi_n$ . Let the distance  $d_n$  defined by  $d_n = |x_n - y_n|$ . The NICS is said to occur if for any  $(x_0, y_0)$  there

exist an integer  $n_0$  such that  $d_n$  ( $n \geq n_0$ ) is smaller than a given small threshold. To examine the NICS in maps (2) and (3), we use the time average

$$\bar{d} = \lim_{N \rightarrow \infty} \frac{1}{N} \sum_{n=0}^{N-1} d_n. \quad (4)$$

The  $\bar{d}$  in general could depend on the realization of  $\xi_n$  and on the initial conditions  $(x_0, y_0)$ . Therefore, we numerically calculate an average of  $\bar{d}$  taken over both ensembles. Figure 2 shows the average  $\bar{d}$  plotted as a function of  $\sigma$ . For each map,  $\bar{d}$  decreases with increasing  $\sigma$  and there is a threshold such that  $\bar{d} = 0$  holds when  $\sigma$  is larger than it.

A more precise and useful criterion for the NICS is based on the *conditional Lyapunov exponent*, which is defined by

$$\lambda = \lim_{N \rightarrow \infty} \frac{1}{N} \sum_{n=0}^{N-1} \ln |f'(x_n)|. \quad (5)$$

The synchronization can occur only if  $\lambda$  is negative [5]. The conditional Lyapunov exponent  $\lambda$  is the average of  $\ln |f'(x_n)|$  found by the trajectory. Slopes  $f' \in (-1, 1)$  contribute to  $\lambda$  with negative values while slopes  $f' \in (-\infty, -1) \cup (1, \infty)$  contribute with positive values. Equation (5) does not explicitly depend on  $\xi_n$  and is of the same form between the noise-free ( $\sigma = 0$ ) and the noisy ( $\sigma \neq 0$ ) cases. Therefore,  $\lambda$  seems not to be modified by the presence of noise. However, the presence of noise modifies the time evolution of the system, in other words, there is noise dependence of  $\lambda$  through the trajectory points  $x_n$ ,  $n = 0, 1, 2, \dots$ . For our examples of maps (2) and (3),  $|f'(x)| < 1$  holds in the regions for large  $|x|$  as seen in Fig. 1. When the noise amplitude  $\sigma$  is small,  $|x_n|$  does not take large values and then the trajectory stays in the region of  $|f'(x)| > 1$  for relatively long time, leading to a positive value of  $\lambda$ . In contrast, as  $\sigma$  increases,  $|x_n|$  comes to take large values more frequently. This results in that the trajectory stays in the region of  $|f'(x)| < 1$  for longer time. Therefore, it is expected that  $\lambda$  decreases from positive to negative as  $\sigma$  increases.

Figure 3 shows  $\lambda$  plotted as a function of  $\sigma$  for maps (2) and (3), respectively. For each map,  $\lambda$  decreases as  $\sigma$  increases and becomes negative when  $\sigma$  is larger than a threshold  $\sigma_c$ . The  $\sigma_c$  are found as  $\sigma_c \simeq 0.58$  for map (2) and  $\sigma_c \simeq 2.7$  for map (3), respectively. These threshold values coincide with those obtained from  $\bar{d}$ . From the above results on  $\bar{d}$  and  $\lambda$ , it may be concluded that for both of the maps (2) and (3) the NICS occurs when  $\sigma > \sigma_c$ .

### 3. Memory decay and mutual information

Consider the noise-driven chaotic map (1). Let  $\rho_n^{(1)}(x)$  and  $\rho_n^{(2)}(x)$  be the probability distributions at time  $n$  with arbitrary initial distributions  $\rho_0^{(1)}(x)$  and  $\rho_0^{(2)}(x)$ , respectively. We assume that the initial distributions have a finite width and are not given by the Dirac's delta function. For the

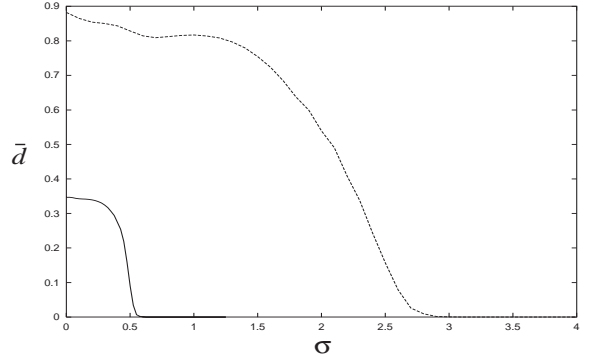


Figure 2: Average distance  $\bar{d}$  for map (2) (solid line) and map (3) (dashed line).

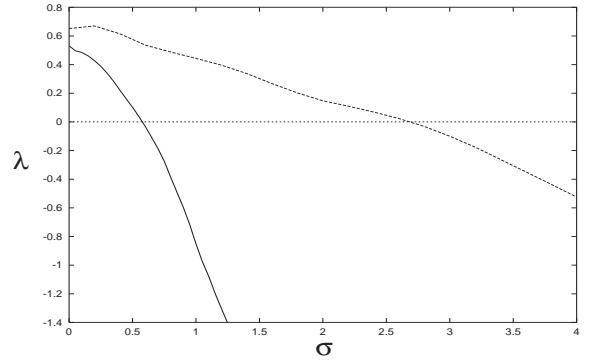


Figure 3: Conditional Lyapunov exponent plotted against noise amplitude for map (2) (solid line) and map (3) (dashed line).

same realization of noise,  $\rho_n^{(1)}(x)$  and  $\rho_n^{(2)}(x)$  converge with each other: i.e.,  $\|\rho_n^{(1)}(x) - \rho_n^{(2)}(x)\| \rightarrow 0$  in the limit  $n \rightarrow \infty$ , where  $\|\cdot\|_1$  represents the  $L^1$  norm. In fact, this convergence property is observed for the maps (2) and (3). We note that the probability distribution does not converge to a static distribution but still depends on time  $n$  due to  $\xi_n$  except for the case  $\sigma = 0$ . We give a rough explanation to this convergence property. Given a noise sequence  $\xi_n$ ,  $n = 0, 1, 2, \dots$ , let  $F_n(x)$  defined by  $F_n(x) = f(x) + \sigma \xi_n$ . We consider the Frobenius-Perron (FP) operator  $P_n$  associated with the transformation  $F_n$ . The FP operator  $P_n : L^1 \rightarrow L^1$  is given by

$$P_n \psi(x) = \sum_{y \in F_n^{-1}(x)} \frac{\psi(y)}{|F_n'(y)|}, \quad (6)$$

where  $\psi(x) \in L^1$ . The FP operator  $P_n$  has the contraction property: i.e.,  $\|P_n \psi\|_1 \leq \|\psi\|_1$  for any  $\psi \in L^1$ . We consider the difference  $\Delta_n(x) = \rho_n^{(1)}(x) - \rho_n^{(2)}(x)$ . By the contraction property of  $P_n$ , we have  $\|\Delta_{n+1}\|_1 = \|P_n \Delta_n\|_1 \leq \|\Delta_n\|_1$ . Hence, we have

$$\|\Delta_0\|_1 \geq \|\Delta_1\|_1 \geq \dots \geq \|\Delta_n\|_1 \geq \dots \quad (7)$$

It is expected that for this type of noise-driven map most of the inequalities are strict in Eq. (7) and  $\|\Delta_n\|_1 \rightarrow 0$  as  $n$  increases.

Let  $\rho_n(x)$  be the probability distribution at time  $n$ , which starts from an arbitrary initial distribution  $\rho_0(x)$  having a finite width. When the NICS occurs, any trajectory  $x_n$  with an arbitrary initial condition converges to a single trajectory  $s_n$ , i.e.,  $|x_n - s_n| \rightarrow 0$  as  $n$  increases. Therefore, in terms of the probability distribution, the NICS is characterized by the convergence of  $\rho_n(x)$  to the Dirac's delta function  $\delta(x - s_n)$  with the time-dependent point  $s_n$  of nonzero probability. In the opposite case  $\sigma = 0$ ,  $\rho_n(x)$  converges to the invariant probability distribution, which is independent of time. In the intermediate case  $0 < \sigma < \sigma_c$ ,  $\rho_n(x)$  is a time-dependent and broadened distribution.

As mentioned above,  $\rho_n(x)$  becomes independent of the initial probability distribution  $\rho_0(x)$  for large  $n$ , provided that  $\rho_0(x)$  is not given by the delta function. This implies that if the initial position  $x_0$  is measured within a finite precision, then this information about the initial position gives no additional information about the position  $x_n$  for large  $n$ . For example, consider the two initial probability distributions  $\rho_0^{(k)}(x)$ ,  $k = 1, 2$  given by

$$\rho_0^{(k)}(x) = \begin{cases} 1/2\varepsilon & \text{if } |x - c_k| \leq \varepsilon, \\ 0 & \text{otherwise,} \end{cases} \quad (8)$$

where  $\varepsilon > 0$  is a small constant and  $c_1 \neq c_2$ . The  $\rho_0^{(k)}(x)$  is the probability distribution centered at  $x = c_k$  with the small width  $2\varepsilon$ . Let  $\rho_n^{(1)}(x)$  and  $\rho_n^{(2)}(x)$  be the probability distributions at time  $n$  starting from  $\rho_0^{(1)}(x)$  and  $\rho_0^{(2)}(x)$ , respectively. For large  $n$ ,  $\rho_n^{(1)}(x)$  and  $\rho_n^{(2)}(x)$  cannot be distinguished if they are measured with a finite resolution.

To quantify the decay of information about the initial conditions, we use the mutual information between the initial positions of trajectories and their positions at time  $n$ . Consider an interval  $\mathcal{I} = [a_1, a_2] \subset \mathbf{R}$  and divide  $\mathcal{I}$  into equal  $M$  subintervals. We denote the  $i$ th subinterval by  $\mathcal{I}_i$ . Let  $X \in \{1, 2, \dots, M\}$  be the stochastic variable representing the index of subintervals  $\mathcal{I}_i$  and  $P_X(i)$  be the probability of finding the initial position  $x_0$  in the  $i$ th subinterval  $\mathcal{I}_i$ , i.e.,  $P_X(i) = \text{Prob}[x_0 \in \mathcal{I}_i] = \int_{\mathcal{I}_i} \rho_0(x) dx$ . Similarly, consider an interval  $\mathcal{J} = [b_1, b_2] \subset \mathbf{R}$  and divide  $\mathcal{J}$  into equal  $N$  subintervals. We denote the  $j$ th subinterval by  $\mathcal{J}_j$  and introduce the stochastic variable  $Y \in \{1, 2, \dots, N\}$ , which represents the index of subintervals  $\mathcal{J}_j$ . We can consider the joint probability  $P_{XY}(i, j)$  defined by  $P_{XY}(i, j) = \text{Prob}[x_0 \in \mathcal{I}_i, x_n \in \mathcal{J}_j]$ , where  $x_n$  is the position at time  $n$  of the trajectory with the initial position  $x_0$ . The mutual information between the stochastic variables  $X$  and  $Y$  is defined by

$$\begin{aligned} I_n &= H(Y) - H(Y|X) \\ &= \sum_{j=1}^N P_Y(j) \log_2 P_Y(j) \end{aligned} \quad (9)$$

$$- \sum_{i=1}^M \sum_{j=1}^N P_{XY}(i, j) \log_2 \frac{P_{XY}(i, j)}{P_X(i)}, \quad (10)$$

where  $H(X)$  and  $H(Y|X)$  are the entropy and the conditional entropy, respectively. The mutual information  $I_n$  is the quantity that measures the amount of information about  $x_n$  obtained by knowing the initial position  $x_0$ . Because of the convergence property of  $\rho_n$ ,  $I_n$  decreases and approaches zero as  $n$  increases.

We define the memory decay time  $T$  as the first instant of time such that  $I_n$  becomes smaller than  $I_c$ , where  $I_c$  is a small threshold. Since  $T$  depends on a given realization of the noise sequence  $\xi_n$ , we use the average of  $T$  taken over multiple realizations of  $\xi_n$ .

#### 4. Numerical results for memory decay time

Figure 4 shows the memory decay time  $T$  plotted as a function of  $\sigma$  for map (2). The numerical results are displayed for three different threshold values  $I_c = 0.10, 0.05$ , and  $0.01$ . In these calculations, we assumed that  $\mathcal{I} = [0, 1]$ ,  $M = 10$ ,  $\mathcal{J} = [-2.5, 2.5]$ ,  $N = 100$ , and  $\rho_0(x)$  uniformly distributed over  $\mathcal{I}$ . The memory decay time  $T$  increases as  $\sigma$  increases up to  $\sigma \simeq 0.60$ , above which it decreases, being maximized at  $\sigma \simeq 0.60$ . This behavior is clearly observed for all of the three curves shown in Fig. 4. The value  $\sigma \simeq 0.60$  for the maximum point well coincides with the transition point to the NICS, which is determined as  $\sigma_c \simeq 0.58$  from the conditional Lyapunov exponent  $\lambda$ .

Figure 5 shows similar results for map (3). In these calculations, we assumed that  $\mathcal{I} = [-2, 2]$ ,  $M = 10$ ,  $\mathcal{J} = [-4, 4]$ ,  $N = 100$ , and  $\rho_0(x)$  uniformly distributed over  $\mathcal{I}$ . In this figure, the same behavior of  $T(\sigma)$  as in Fig. 4 is clearly observed: the memory decay time  $T$  increases as  $\sigma$  increases up to  $\sigma \simeq 2.7$ , above which it decreases, being maximized at  $\sigma \simeq 2.7$ . The value of  $\sigma$  for the maximum point coincides with the transition point to the NICS, which is determined as  $\sigma_c \simeq 2.7$  from  $\lambda$ , also using the map (3).

Based on the numerical results in Figs. 4 and 5, we may conclude that the memory decay time is maximized at the point of transition to the NICS. This is an example of an anomalous behavior, which can occur at a transition point to the NICS, and may be observed in the other chaotic systems exhibiting the NICS.

We give a qualitative explanation of the above numerical observations. We first consider the case  $\sigma_c < \sigma$ . As shown in Fig. 3,  $\lambda$  is negative and decreases with increasing  $\sigma$  when  $\sigma_c < \sigma$ . This implies that the probability distribution  $\rho_n(x)$  shrinks to the asymptotic form  $\delta(x - s_n)$  more rapidly as  $\sigma$  increases. Therefore, the memory about the initial conditions also decays more rapidly as  $\sigma$  increases. We turn to the case  $0 \leq \sigma < \sigma_c$ . In this range of  $\sigma$ ,  $\lambda$  is positive and increases with decreasing  $\sigma$ . This implies that for smaller  $\sigma$  a local segment of  $\rho_n(x)$  tends to be mapped to a more broad segment at each iteration. In other words,

the map has a stronger mixing property for smaller  $\sigma$ . This results in more rapid decay of the memory about the initial condition as  $\sigma$  decreases. At the transition point  $\sigma = \sigma_c$ , these two effects, the mixing effect and the synchronization effect, are balanced and then the memory decay time becomes long.

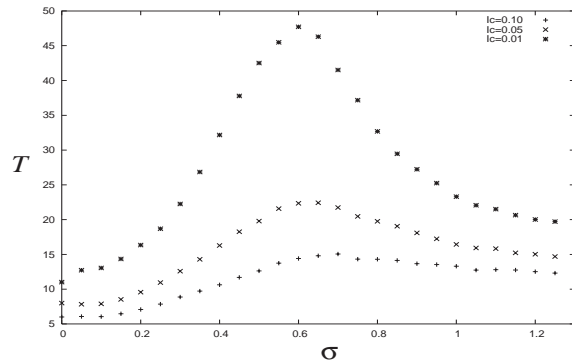


Figure 4: Memory decay time plotted against noise amplitude for map (2). Results for three different thresholds are plotted:  $I_c = 0.10$ ,  $0.05$ , and  $0.01$ .

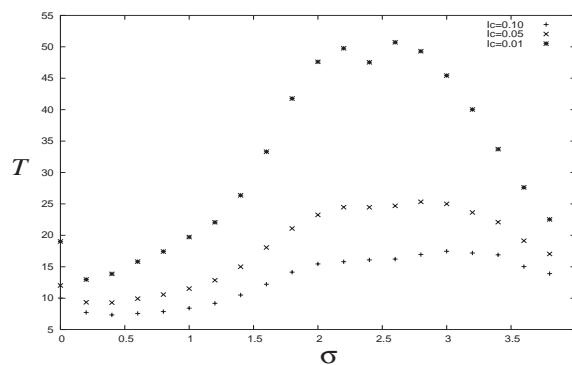


Figure 5: Memory decay time plotted against noise amplitude for map (3). Results for three different thresholds are plotted:  $I_c = 0.10$ ,  $0.05$ , and  $0.01$ .

## 5. Conclusions

We studied the memory decay time in one-dimensional chaotic maps that exhibit the NICS. It was shown that the memory decay time becomes maximum at the transition to the NICS. We gave a qualitative explanation to the reason why the memory decay time is maximized at the transition point.

## Acknowledgment

The authors would like to thank the members of NTT Communication Science Laboratories for their continual

encouragement.

## References

- [1] K. Matsumoto and I. Tsuda, *J. of Phys. A*, vol.18, pp.3561-3566, 1985.
- [2] K. Matsumoto and I. Tsuda, *Physica D*, vol.26, pp.347-357, 1987.
- [3] R. Toral, C. R. Mirasso, E. Hernández-García, and O. Piro, *Chaos*, vol.11, pp.665-673, 2001.
- [4] L. Baroni, R. Livi, and A. Torcini, *Phys. Rev. E*, vol.63, 036226, 2001.
- [5] A. S. Pikovsky, *Phys. Lett. A*, vol.165, pp.33-36, 1992.